

Hot Carrier Effects on Real and Imaginary Parts of Brillouin Susceptibilities of Magnetoactive Doped III-V Semiconductors (Applied to N-type Doped InSb)

Renu Kumari^{1,*} and Manjeet Singh²

¹Department of Physics, Singhania University, Rajasthan 333515, India

²Department of Physics, Government College Matanhail Jhajjar, Haryana 124106, India

(*Corresponding author's e-mail: renu.singhaniauniv@gmail.com)

Received: 20 July 2021, Revised: 22 August 2021, Accepted: 29 August 2021

Abstract

An analytical investigation is made of hot carrier effects on real and imaginary parts of Brillouin susceptibility ($\text{Re}, \text{Im}(\chi_B)$) of magnetoactive doped III-V semiconductors. Coupled mode approach is used to obtain expressions for $\text{Re}, \text{Im}(\chi_B)$. Numerical calculations are made for n-InSb crystal CO_2 laser system. Efforts are made to obtain enhanced values of $\text{Re}, \text{Im}(\chi_B)$ and change of their sign under appropriate selection of external magnetic field (B_0) and doping concentration (n_0). The hot carrier effects of intense laser radiation modifies the momentum transfer collision frequency of carriers and consequently the nonlinearity of the medium, which in turn (i) further enhances $\text{Re}, \text{Im}(\chi_B)$, (ii) shifts the enhanced $\text{Re}, \text{Im}(\chi_B)$ towards smaller values of B_0 , and (iii) widens the range of B_0 at which change of sign of $\text{Re}, \text{Im}(\chi_B)$ occurs. The change of sign of enhanced $\text{Re}, \text{Im}(\chi_B)$ of magnetoactive doped III-V semiconductors, validates the possibility of chosen Brillouin medium as a potential candidate material for the fabrication of stimulated Brillouin scattering dependent widely tunable and efficient optoelectronic devices such as optical switches and frequency converters.

Keywords: Brillouin susceptibility, Carrier heating, Doping, Magnetic field, III-V semiconductors

Introduction

The studies of nonlinear optical susceptibilities provide the important information of the nonlinearity of a medium and impart an extensive role in the fabrication of various optoelectronic devices [1-3]. In addition, the change of sign of nonlinear optical susceptibilities exhibit interesting nonlinear optical phenomena [4,5]. The selection and operating frequency of a medium are the essential features in designing the optoelectronic devices. Out of various nonlinear media, the III-V semiconductors offer greater flexibility in fabrication of optoelectronic devices. This is due to their compactness, provision of control of (electrons/holes) carriers relaxation time via materials designing and device structuring, operation of the devices under either oblique/normal incidence or in waveguide structures, highly advanced fabrication technology, and integrating the devices with other optoelectronic components [6]. In addition, these crystals exhibit large magnitude nonlinear optical susceptibilities in close proximity to the band-gap resonant transition regimes [7]; which can be further enhanced by application of external electric/magnetic fields [8-10]. Thus, the selection of doped semiconductors as nonlinear media for the study of nonlinear optical phenomena is unquestionable.

Out of various nonlinear optical phenomena, the study of stimulated Brillouin scattering (SBS) is currently a major field of research due to its vast potentiality over a broad range of optoelectronic devices [11,12]. SBS occurs due to scattering of a laser radiation by acoustical vibrational mode of the medium. It is a third-order optical phenomenon and its origin lies in third-order (Brillouin) susceptibility of the medium. In the past, various aspects of Brillouin susceptibilities of magnetoactive doped III-V semiconductors have been explored to study SBS and related phenomena by research group of one of the present authors [13-16] and others [17]. Keeping in mind the overall performance of SBS based optoelectronic devices, the knowledge of Brillouin susceptibility of doped III-V semiconductors and its characteristic dependence on various factors affecting it is essential [18].

It comes out from literature survey that no theoretical formulation has been made till now to explore the influence of hot carrier effects (HCEs) on Brillouin susceptibility of magnetoactive doped III-V semiconductors. In the present paper, we develop a theoretical formulation followed by numerical analysis to study HCEs of intense laser radiation on real and imaginary parts of Brillouin susceptibility of magnetoactive doped III-V semiconductors (acting as Brillouin media). The motivation for this study arises from the fact that HCEs of intense laser radiation may remarkably modify the nonlinearity of the medium and consequently the SBS process. Under high-power laser irradiation, this investigation becomes more important as it leads to better understanding of SBS in magnetoactive doped III-V semiconductors. Considering the origin of the phenomenon to lie in finite nonlinear induced polarization (due to acoustical vibrational mode-laser radiation coupling) and using the coupled mode theory of interacting waves, expressions for real and imaginary parts of Brillouin susceptibility of magnetoactive doped III-V semiconductors are obtained under hydrodynamic approximation. Efforts are made to optimize the doping level and to find appropriate values of external magnetic field to enhance magnitudes of Brillouin susceptibilities and alter of their sign for applications in efficient optoelectronic devices, such as optical switches, frequency converters etc. Finally, complete numerical analysis is made with a set of data available for *n*-InSb illuminated by a pulsed CO₂ laser.

Materials and methods

In this section, expressions are obtained for real and imaginary parts of Brillouin susceptibility (Re, Im(χ_B)) of magnetoactive doped III-V semiconductors under hydrodynamic approximation [19] $k_a l \ll 1$, where k_a is the acoustical vibrational wave number, and l is the carriers mean free path. SBS occurs due to nonlinear interaction among 3 coherent fields in a Brillouin medium, viz. an intense laser radiation field $E_0(x, t) = E_0 \exp[i(k_0 x - \omega_0 t)]$, an induced acoustical vibrational mode $u(x, t) = u_0 \exp[i(k_a x - \omega_a t)]$, and scattered Stokes component of incident laser radiation field $E_s(x, t) = E_s \exp[i(k_s x - \omega_s t)]$. These fields are connected by energy and momentum phase matching constraints $\hbar\omega_0 = \hbar\omega_a + \hbar\omega_s$ and $\hbar\vec{k}_0 = \hbar\vec{k}_a + \hbar\vec{k}_s$, respectively. The Brillouin medium is subjected to an external magnetic field $\vec{B}_0 = \hat{z}B_0$ (i.e. perpendicular to wave vectors \vec{k}_0 , \vec{k}_a and \vec{k}_s). This configuration is known as Voigt geometry [20].

The basic equations used in the formulation of Re, Im(χ_B) are:

$$\frac{\partial^2 u(x, t)}{\partial t^2} = \frac{C}{\rho} \frac{\partial^2 u(x, t)}{\partial x^2} - 2\Gamma_a \frac{\partial u(x, t)}{\partial t} - \frac{\beta}{\rho} \frac{\partial E_1}{\partial x} + \frac{\gamma}{2\rho} \frac{\partial}{\partial x} (E_0 E_1^*) \tag{1}$$

$$\frac{\partial \vec{v}_0}{\partial t} + v_0 \vec{v}_0 + \left(\vec{v}_0 \cdot \frac{\partial}{\partial x} \right) \vec{v}_0 = -\frac{e}{m} [\vec{E}_0 + (\vec{v}_0 \times \vec{B}_0)] = -\frac{e}{m} (\vec{E}_e) \tag{2}$$

$$\frac{\partial \vec{v}_1}{\partial t} + v_0 \vec{v}_1 + \left(\vec{v}_0 \cdot \frac{\partial}{\partial x} \right) \vec{v}_1 + \left(\vec{v}_1 \cdot \frac{\partial}{\partial x} \right) \vec{v}_0 = -\frac{e}{m} [\vec{E}_1 + (\vec{v}_0 \times \vec{B}_0)] \tag{3}$$

$$\frac{\partial n_1}{\partial t} + n_0 \frac{\partial v_1}{\partial x} + n_1 \frac{\partial v_0}{\partial x} + v_0 \frac{\partial n_1}{\partial x} = 0 \tag{4}$$

$$\vec{P}_{es} = -\gamma \frac{\partial u}{\partial x} (\vec{E}_0) \tag{5}$$

$$\frac{\partial E_{sc}}{\partial x} + \frac{\beta}{\varepsilon} \frac{\partial^2 u}{\partial x^2} + \frac{\gamma}{\varepsilon} \frac{\partial^2 u^*}{\partial x^2} (E_0) = -\frac{n_1 e}{\varepsilon} \tag{6}$$

These equations have been used in analytical investigations of SBS in magnetoactive doped III-V semiconductors by research group of one of the present authors [13-16]. Here, C represents the elastic stiffness constant of the Brillouin medium such that the speed of acoustical vibrational mode is given by

$v_a = (C/\rho)^{1/2}$. ρ is the mass density of Brillouin medium. In order to take account of acoustical damping, the term $2\Gamma_a \partial u(x,t)/\partial t$ is introduced in Eq. (1) phenomenologically. In Eq. (1), β and γ are the piezoelectric and electrostrictive coefficients of the Brillouin medium, respectively. Here, these coefficients are used phenomenologically; their effect on parametric and Brillouin nonlinearities of magnetoactive doped III-V semiconductors is available in literature [13]. E_1 represents the perturbed electric field and E_{sc} stands for space charge electric field. n_0 (\bar{v}_0) and n_1 (\bar{v}_1) represent the carrier's equilibrium and perturbed concentrations (oscillatory fluid velocities), respectively. ν_0 stands for momentum transfer collision frequency (MTCF) of electrons. m is the effective mass of an electron. P_{es} is the polarization originating via electrostrictive property of the Brillouin medium. The asterisk (*) represents the conjugate of a complex entity.

The x - and y -components of equilibrium carrier's fluid velocity are obtained from Eq. (2) as:

$$v_{0x} = \frac{e(\nu + i\omega_0)}{m(\omega_c^2 - \omega_0^2 + 2i\nu\omega_0)} E_0, \tag{7a}$$

And

$$v_{0y} = \frac{\omega_c}{(\nu + i\omega_0)} v_{0x}. \tag{7b}$$

In Eqs. (7a) - (7b), $\omega_c = (e/m)B_0$ is the electron-cyclotron frequency.

The x - and y -components of perturbed carrier's fluid velocity can be obtained from Eq. (3) by using the method adopted by Sharma and Ghosh [21]:

$$v_{1x} = \frac{\nu}{(\nu^2 + \omega_c^2)} \left[\bar{E} - ik_0 \left(\frac{k_B T_0}{m n_0} \right) n_1 \right], \tag{8a}$$

And

$$v_{1y} = \frac{\omega_c}{(\nu^2 + \omega_c^2)} \left[-\bar{E} + ik_0 \left(\frac{k_B T_0}{m n_0} \right) n_1 \right]. \tag{8b}$$

In Eqs. (8a) - (8b), $\bar{E} = (e/m)|\vec{E}_e|$, T_0 is temperature of Brillouin medium, and k_B is Boltzmann's constant.

In order to excite SBS, the basic need is to irradiate the Brillouin sample by an intense laser. Under the influence of laser radiation field, the electrons (which are mobile charge carriers in n-type doped semiconductor) gain energy and their temperature reaches a value $T_e (> T_0)$. Consequently, the MTCF of electrons modifies via relation [22]:

$$\nu = \nu_0 \left(\frac{T_e}{T_0} \right)^{1/2}. \tag{9}$$

In Eq. (9), the value of T_e/T_0 can be determined from energy conservation relation under steady-state operation. Following Sodha *et al.* [23] and using Eqs. (7a) - (7b), the time independent part of power absorbed by a single mobile charge carrier (here electron) from the laser radiation field is given by:

$$\frac{e}{2} \text{Re}(v_{0x}^{\text{r}} \cdot E_e^{\text{r}*}) = \frac{e^2 \nu_0}{2m} \frac{(\omega_c^2 - \omega_0^2)}{[(\omega_c^2 - \omega_0^2)^2 + 4\nu_0^2 \omega_0^2]} |E_0^{\text{r}}|^2, \tag{10}$$

where $\text{Re}(v_{0x} \cdot \vec{E}_e^*)$ denotes the real part of the quantity $(v_{0x} \cdot \vec{E}_e^*)$.

Following Conwell [24], the power dissipated by a single electron from the laser radiation field in collisions with polar optical phonons (POPs) is given by:

$$\left(\frac{\partial \epsilon}{\partial t}\right)_{diss} = eE_{po}(x_0)^{1/2} \kappa_0 \left(\frac{2k_B\theta_D}{m\pi}\right)^{1/2} \left(\frac{x_e}{2}\right) \cdot \exp\left(\frac{x_e}{2}\right) \cdot \frac{\exp(x_0 - x_e) - 1}{\exp(x_0) - 1}, \tag{11}$$

where $x_{0,e} = \frac{h\omega_l}{k_B T_{0,e}}$, in which $h\omega_l$ is the energy possessed by POPs given by $h\omega_l = k_B\theta_D$, where θ_D is

the Debye temperature of the Brillouin medium. $E_{po} = \frac{meh\omega_l}{h^2} \left(\frac{1}{\epsilon_\infty} - \frac{1}{\epsilon}\right)$ represents the POPs scattering potential field, in which ϵ and ϵ_∞ are the static and high frequency dielectric constant of the Brillouin medium.

Under steady-state operation, the power absorbed by a single electron from the laser radiation field is exactly equal to the power dissipated by it in collisions with POPs. Consequently, the electron-plasma attains a steady temperature $T_e (> T_0)$. In case of average heating of the electrons-plasma, Eqs. (10) - (11) yield:

$$\frac{T_e}{T_0} = 1 + \alpha \left| \vec{E}_0 \right|^2, \tag{12}$$

where $\alpha = \frac{e^2 v_0}{2m\tau\Omega_0^2} \frac{(\omega_c^2 - \omega_0^2)}{[(\omega_c^2 - \omega_0^2)^2 + 4v_0^2\omega_0^2]}$, in which $\tau = eE_{po}\kappa_0 \left(\frac{2k_B\theta_D}{m\pi}\right)^{1/2} \left(\frac{x_0}{2}\right) \frac{(x_0)^{1/2} \exp(x_0/2)}{\exp(x_0) - 1}$.

Using Eqs. (9) - (11), the modified MTCF of electrons is given by:

$$v = v_0 \left(1 + \alpha \left| \vec{E}_0 \right|^2\right)^{1/2} \approx v_0 \left(1 + \frac{1}{2} \alpha \left| \vec{E}_0 \right|^2\right). \tag{13}$$

The laser radiation induces perturbations in electrons concentration in the Brillouin medium via piezoelectric and electrostrictive strains. The coupled equation of these perturbations, including HCEs, can be obtained by using the standard approach [25]. Differentiating Eq. (4), substitute the value of E_1 from Eq. (6), first-order derivatives of v_0 and v_1 from Eqs. (2) - (3), respectively and after mathematical simplification, we obtain

$$\frac{\partial^2 n_1}{\partial t^2} + v \frac{\partial n_1}{\partial t} + \bar{\omega}_p^2 n_1 + \frac{n_0 e k_s^2 u^* (\beta \gamma \delta_1 \delta_2 A + \gamma^2 E_0^2)}{m \epsilon_1} E_0 E_s^* = i n_1 k_s \bar{E}, \tag{14}$$

where $A = \frac{\omega_p^2}{(e/m)k_a}$, $\bar{\omega}_p = \frac{v\omega_p}{(v^2 + \omega_c^2)^{1/2}}$, $\delta_1 = 1 - \frac{\omega_c^2}{(\omega_0^2 - \omega_c^2)}$, $\delta_2 = 1 - \frac{\omega_c^2}{(\omega_s^2 - \omega_c^2)}$, and $\omega_p = \left(\frac{n_0 e^2}{m\epsilon}\right)^{1/2}$ (electron-plasma frequency).

The perturbed electron concentration (n_1) may be put forward as: $n_1 = n_{1s}(\omega_a) + n_{1f}(\omega_s)$, where n_{1s} and n_{1f} are known as low- and high-frequency components; oscillate at acoustical vibrational mode frequency ω_a and electromagnetic waves at frequencies $\omega_0 \pm p\omega_a$, in which $p = 1, 2, 3, \dots$, respectively. The electromagnetic fields at sum (i.e. $\omega_0 + p\omega_a$) and difference frequencies (i.e. $\omega_0 - p\omega_a$) are termed as anti-Stokes and Stokes modes, respectively. In the present analysis, the electron concentration perturbations at off-resonant frequencies (with $p \geq 2$) are neglected and only the first-order Stokes mode

(with $p = 1$) is considered [14]. Under rotating-wave approximation (RWA), Eq. (14) lead to following coupled wave equations:

$$\frac{\partial^2 n_{1f}}{\partial t^2} + v \frac{\partial n_{1f}}{\partial t} + \bar{\omega}_p^2 n_{1f} + \frac{n_0 e k_s^2 u^* (\beta \gamma \delta_1 \delta_2 A + \gamma^2 E_0^2)}{m \varepsilon} E_0 E_s^* = -i n_{1s}^* k_s \bar{E} \quad (15a)$$

And

$$\frac{\partial^2 n_{1s}}{\partial t^2} + v \frac{\partial n_{1s}}{\partial t} + \bar{\omega}_p^2 n_{1s} = i n_{1f}^* k_s \bar{E}. \quad (15b)$$

Eqs. (15a) - (15b) manifest that both n_{1s} and n_{1f} are coupled to each other via laser radiation field (\bar{E}). Thus, it clearly illustrates that for SBS to take place, the presence of the laser radiation field is the pre-requisite condition.

Solving Eqs. (15a) - (15b) and using Eq. (1), an expression for n_{1s} may be obtained as:

$$n_{1s} = \frac{\varepsilon_0 n_0 k_a k_s (\beta \gamma \delta_1 \delta_2 A + \gamma^2 E_0^2)}{2\rho \varepsilon \delta_3 (\Omega_a^2 + 2i\Gamma_a \omega_a)(\omega_0^2 - \omega_c^2 + 2iv\omega_0)} E_0 E_s^*, \quad (16)$$

where $\Omega_a^2 = \omega_a^2 - k_a^2 v_a^2$, $\delta_3 = 1 - \frac{(\Omega_{ps}^2 - iv\omega_s)(\Omega_{pa}^2 + iv\omega_a)}{k_s^2 \bar{E}^2}$, in which $\Omega_{ps}^2 = \bar{\omega}_p^2 - \omega_s^2$, $\Omega_{pa}^2 = \bar{\omega}_p^2 - \omega_a^2$.

The induced current density (J_{cd}) of the Brillouin medium at Stokes frequency (ω_s), including HCEs, is obtained (by neglecting transition dipole moment) as:

$$J_{cd}(\omega_s) = n_{1s}^* e v_0 = \frac{\varepsilon_0 k_a k_s \omega_p^2 (v - i\omega_0) (\beta \gamma \delta_1 \delta_2 A + \gamma^2 E_0^2)}{2\rho \delta_3 (\Omega_a^2 + 2i\Gamma_a \omega_a)(\omega_0^2 - \omega_c^2 + 2iv\omega_0)} |E_0|^2 E_s^*. \quad (17)$$

The nonlinear induced polarization of the Brillouin medium (which is time integral of induced current density), including HCEs, is obtained as:

$$P_{cd}(\omega_s) = \int J_{cd}(\omega_s) dt = \frac{\varepsilon_0 k_a k_s \omega_p^2 \omega_0^3 (\beta \gamma \delta_1 \delta_2 A + \gamma^2 E_0^2)}{2\rho \omega_s \delta_3 (\Omega_a^2 + 2i\Gamma_a \omega_a)(\omega_0^2 - \omega_c^2 + 2iv\omega_0)} |E_0|^2 E_s^*. \quad (18)$$

Besides $P_{cd}(\omega_s)$, the Brillouin medium also possesses a polarization $P_{es}(\omega_s)$ originating via electrostrictive property of the Brillouin medium. Following Ref. [14], and using Eqs. (1) - (5), we obtain:

$$P_{es}(\omega_s) = \frac{k_a k_s \omega_0^4 \gamma^2}{2\rho (\Omega_a^2 + 2i\Gamma_a \omega_a)(\omega_0^2 - \omega_c^2 + 2iv\omega_0)} |E_0|^2 E_s^*. \quad (19)$$

Using Eqs. (18) - (19), the effective nonlinear induced polarization of Brillouin medium, including HCEs, is given by:

$$P(\omega_s) = P_{cd}(\omega_s) + P_{es}(\omega_s) = \frac{k_a k_s \omega_0^3 [\varepsilon_0 \omega_p^2 (\beta \gamma \delta_1 \delta_2 A + \gamma^2 E_0^2) + \delta_3 \omega_s \omega_0 \gamma^2]}{2\rho \delta_3 \omega_s (\Omega_a^2 + 2i\Gamma_a \omega_a)(\omega_0^2 - \omega_c^2 + 2iv\omega_0)} |E_0|^2 E_s^*. \quad (20)$$

Consequently, the effective Brillouin susceptibility of the Brillouin medium, including HCEs, is given by:

$$\chi_B = \frac{k_a k_s \omega_0^3 [\varepsilon_0 \omega_p^2 (\beta \gamma \delta_1 \delta_2 A + \gamma^2 E_0^2) + \delta_3 \omega_s \omega_0 \gamma^2]}{2\rho \varepsilon_0 \delta_3 \omega_s (\Omega_a^2 + 2i\Gamma_a \omega_a)(\omega_0^2 - \omega_c^2 + 2iv\omega_0)} \quad (21)$$

Eq. (21) reveals that χ_B is a complex quantity and it can be put forward as: $\chi_B = \text{Re}(\chi_B) + i \text{Im}(\chi_B)$, where $\text{Re}(\chi_B)$ and $\text{Im}(\chi_B)$ stand for real and imaginary parts of complex χ_B . Rationalizing Eq. (21), we obtain:

$$\text{Re}(\chi_B) = \frac{k_a k_s \omega_0^3 [\Omega_a^2 (\omega_0^2 - \omega_c^2) - 4v\Gamma_a \omega_a \omega_0] [\varepsilon_0 \omega_p^2 (\beta \gamma \delta_1 \delta_2 A + \gamma^2 E_0^2) + \delta_3 \omega_s \omega_0 \gamma^2]}{2\rho \varepsilon_0 \delta_3 \omega_s (\Omega_a^4 + 4\Gamma_a^2 \omega_a^2) [(\omega_0^2 - \omega_c^2)^2 + 4v^2 \omega_0^2]} \quad (22a)$$

$$\text{Im}(\chi_B) = -\frac{k_a k_s \omega_0^3 [v\omega_0 \Omega_a^2 + \Gamma_a \omega_a (\omega_0^2 - \omega_c^2)] [\varepsilon_0 \omega_p^2 (\beta \gamma \delta_1 \delta_2 A + \gamma^2 E_0^2) + \delta_3 \omega_s \omega_0 \gamma^2]}{\rho \varepsilon_0 \delta_3 \omega_s (\Omega_a^4 + 4\Gamma_a^2 \omega_a^2) [(\omega_0^2 - \omega_c^2)^2 + 4v^2 \omega_0^2]} \quad (22b)$$

Eqs. (22a) - (22b) show that both $\text{Re}(\chi_B)$ as well as $\text{Im}(\chi_B)$ are influenced by β , γ , n_0 (via ω_p), and B_0 (via ω_c). $\text{Im}(\chi_B)$ account for nonlinear absorption coefficient while $\text{Re}(\chi_B)$ account for nonlinear index of refraction of the chosen Brillouin medium. The knowledge of nonlinear absorption coefficient and index of refraction of the Brillouin medium provide the information regarding the design of various optoelectronic devices including amplifiers, oscillators, filters, and couplers [26].

Results and discussion

In order to make the numerical analysis, we choose n-type doped InSb crystal at 77g temperature as a Brillouin medium and illuminated it by a pulsed CO₂ laser at 10.6 μm wavelength. At 77g temperature, the absorption coefficient of chosen Brillouin medium is negligible (around 10 μm wavelength) and the effects of band-to-band transitions can be ignored safely [27]. The material parameters of n-InSb-CO₂ laser system are as follows [14]: $m = 0.014m_0$; m_0 is the electron's rest mass, $\rho = 5.8 \times 10^3 \text{ kg m}^{-3}$, $\varepsilon = 17.8$, $\varepsilon_\infty = 15.68$, $v_a = 4 \times 10^3 \text{ ms}^{-1}$, $\beta = 0.054 \text{ Cm}^{-2}$, $\gamma = 5 \times 10^{10} \text{ s}^{-1}$, $\Gamma_a = 2 \times 10^{10} \text{ s}^{-1}$, $v_0 = 3.5 \times 10^{11} \text{ s}^{-1}$, $\omega_a = 2 \times 10^{11} \text{ s}^{-1}$, $\omega_0 = 1.78 \times 10^{14} \text{ s}^{-1}$, $T_0 = 77\text{g}$, $\theta_D = 278\text{g}$.

Eqs. (22a) - (22b) represent $\text{Re}, \text{Im}(\chi_B)$ of the Brillouin medium with including HCEs. The expressions for $\text{Re}, \text{Im}(\chi_B)$ of the Brillouin medium with excluding HCEs can be obtained by simply replacing v by v_0 (at $T_e = T_0$) in these equations. The dependence of $\text{Re}, \text{Im}(\chi_B)$ on external magnetic field B_0 (via ω_c) and doping concentration n_0 (via ω_p) with excluding and including HCEs are explored. Aim is targeted at: (i) determination of appropriate values of B_0 and n_0 to enhance $\text{Re}, \text{Im}(\chi_B)$, and (ii) searching the usefulness of optoelectronic devices based on Brillouin nonlinearities.

In **Figures (1a)** and **(1b)**, $\text{Re}, \text{Im}(\chi_B)$ are plotted versus magnetic field B_0 for the cases: (i) without HCEs, and (ii) with HCEs. These clearly show the substantial enhancements of $\text{Re}, \text{Im}(\chi_B)$ as well as alter of their sign. The situation at which $\text{Re}, \text{Im}(\chi_B)$ alter their sign is known as 'cut-off' or 'dielectric anomaly' [28].

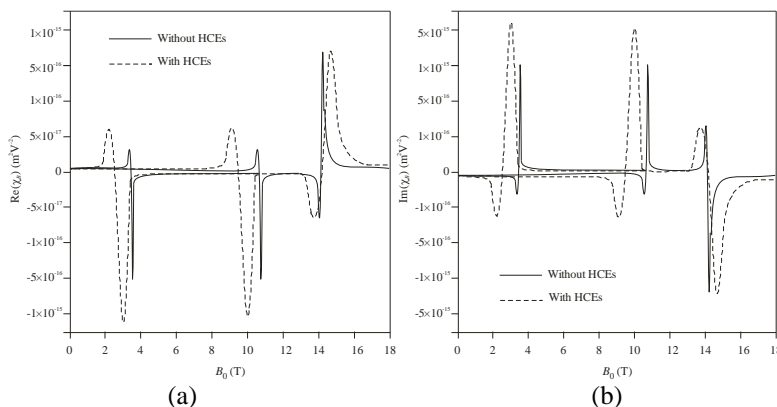


Figure 1 (a); Variation of $\text{Re}(\chi_B)$ versus B_0 for the cases: (i) without HCEs, (ii) with HCEs for $n_0 = 10^{23} \text{ m}^{-3}$, $V = 10^6 \text{ Vm}^{-1}$ and (b); Variation of $\text{Im}(\chi_B)$ versus B_0 for the cases (i), (ii) parameters given in **Figure 1a**.

When HCEs are excluded, with rising B_0 , $\text{Re}(\chi_B)$ is positive while $\text{Im}(\chi_B)$ is negative, vanishingly small, and remain independent of magnetic field for $0 \leq B_0 \leq 2.5 \text{ T}$. The nature of the curves of both $\text{Re}, \text{Im}(\chi_B)$ are very sensitive in the regime $2.5 \text{ T} < B_0 < 4.5 \text{ T}$. In this regime, with rising B_0 , $\text{Re}(\chi_B)$ starts increasing while $\text{Im}(\chi_B)$ starts decreasing achieving a peak positive value ($\text{Re}(\chi_B) = 3 \times 10^{-17} \text{ m}^2 \text{V}^{-2}$) and a peak negative value ($\text{Im}(\chi_B) = -6 \times 10^{-17} \text{ m}^2 \text{V}^{-2}$), respectively at $B_0 = 3.4 \text{ T}$. With slightly rising B_0 beyond this value, $\text{Re}(\chi_B)$ starts sharply decreasing while $\text{Im}(\chi_B)$ starts sharply increasing. At $B_0 = 3.5 \text{ T}$, both $\text{Re}, \text{Im}(\chi_B)$ vanish. With further slightly rising B_0 beyond this value, both $\text{Re}, \text{Im}(\chi_B)$ alter their sign achieving a peak negative value ($\text{Re}(\chi_B) = -6 \times 10^{-16} \text{ m}^2 \text{V}^{-2}$) and peak positive value ($\text{Im}(\chi_B) = 2 \times 10^{-15} \text{ m}^2 \text{V}^{-2}$), respectively at $B_0 = 3.6 \text{ T}$. For $3.6 \text{ T} < B_0 < 4.5 \text{ T}$, $\text{Re}(\chi_B)$ increases sharply while $\text{Im}(\chi_B)$ decreases sharply. For $4.5 \text{ T} \leq B_0 \leq 10 \text{ T}$, $\text{Re}(\chi_B)$ remains negative while $\text{Im}(\chi_B)$ remains positive and vanishingly small. The nature of the curves of both $\text{Re}, \text{Im}(\chi_B)$ is again repeated in the regime $10.8 \text{ T} < B_0 < 11.8 \text{ T}$ like the regime $2.5 \text{ T} < B_0 < 4.5 \text{ T}$. For the regime $11.8 \text{ T} \leq B_0 \leq 13.2 \text{ T}$, $\text{Re}(\chi_B)$ remains negative while $\text{Im}(\chi_B)$ remains positive and vanishingly small. This distinct behavior of $\text{Re}, \text{Im}(\chi_B)$ occur due to following resonance conditions: (i) $(\omega_p^2 \omega_c^2) / v^2 \sim \omega_s^2$, and (ii) $v^2 \omega_p^2 / (v^2 + \omega_c^2) \sim \omega_s^2$. An important aspect of these resonance conditions is the interaction between electron-plasmon mode and electron-cyclotron mode. Let us define this as coupled plasmon-cyclotron mode. When the laser radiation field interacts with this coupled mode, as a consequence, the coupled mode frequency dependent Stokes mode is generated. Here, it is beneficial to shift the scattered Stokes mode frequency to an achievable spectral regime in proportion to ω_p (or n_0) for fixed ω_c (or B_0), ω_c (or B_0) for fixed ω_p (or n_0), and combination of ω_c and ω_p both. By continuously increasing n_0 (via ω_p) and decreasing B_0 (via ω_c) in the same proportion maintains the resonance conditions at a fixed value of ω_s . Further, by continuously increasing n_0 and decreasing B_0 without maintaining their proportion shifts the value of ω_s . At $B_0 = 14.2 \text{ T}$, the change of sign of both $\text{Re}, \text{Im}(\chi_B)$ is observed due to resonance condition: (iii) $\omega_c^2 \sim \omega_0^2$. This resonance condition is independent of ω_p (or n_0).

When HCEs are included, the features of $\text{Re}(\chi_B) - B_0$ and $\text{Im}(\chi_B) - B_0$ plots remain unchanged except that:

- 1) The change of sign of $\text{Re}, \text{Im}(\chi_B)$ which previously occurring at $B_0 = 3.5 \text{ T}$ and 10.8 T have now been shifted to $B_0 = 2.5 \text{ T}$ and 9.8 T , respectively;
- 2) The peak positive and negative values of $\text{Re}, \text{Im}(\chi_B)$ occurring due to resonance conditions (i) and (ii) has been enhanced almost 5 times;
- 3) The range of B_0 at which the change of sign of $\text{Re}, \text{Im}(\chi_B)$ occurs has been widened.
- 4) The magnitude of $\text{Re}, \text{Im}(\chi_B)$ remains unaltered at resonance condition (iii) with including HCEs; rather this resonance condition shifts the value of B_0 at which resonance occurs towards lower values and widens the range of B_0 at which change of sign of both $\text{Re}, \text{Im}(\chi_B)$ occur.

Around resonances, the electron's drift velocity (which is the function of B_0) increases, attains a value higher than acoustical vibrational mode and due to this the rate of energy flow from laser radiation field to acoustical vibrational mode increases, and consequently the amplification of acoustical vibrational mode takes place in the Brillouin medium. Eventually, the interaction between laser radiation field and amplified acoustical vibrational mode enhances the amplitude of scattered Stokes mode.

The most significant feature of the result is monitoring of $\text{Re}, \text{Im}(\chi_B)$ by properly selecting B_0 and also attaining large values of $\text{Re}, \text{Im}(\chi_B)$ in a Brillouin medium consisting of III-V semiconductors. The results obtained in **Figures (1a)** and **(1b)** permit the tuning of scattered Stokes mode over a broad frequency regime and reveal the opportunity of fabrication of frequency converters.

The magnetostatic field considered in the present numerical analysis ($0 \leq B_0 \leq 18$ T) is easily attainable in the laboratory. It should be worth pointing out that Generazio and Spector [29] studied the free carrier absorption for n-InSb-CO₂ and n-InSb-CO laser systems at 77 g by placing the sample in an external magnetostatic field $B_0 \leq 20$ T.

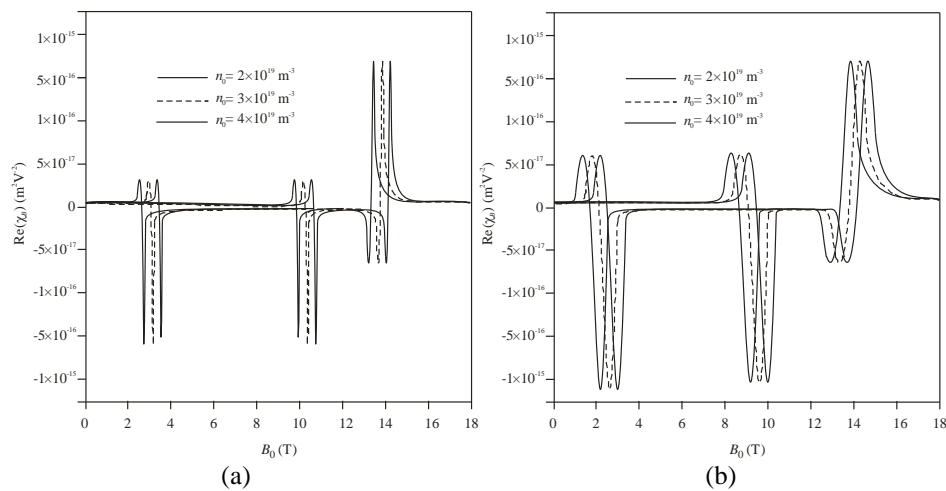


Figure 2 (a); Variation of $\text{Re}(\chi_B)$ versus B_0 with excluding HCEs for 3 different doping concentration (m^{-3} , m^{-3} and m^{-3}) at Vm^{-1} and (b); Variation of $\text{Re}(\chi_B)$ versus B_0 with including HCEs for the parameters given in **Figure (2a)**.

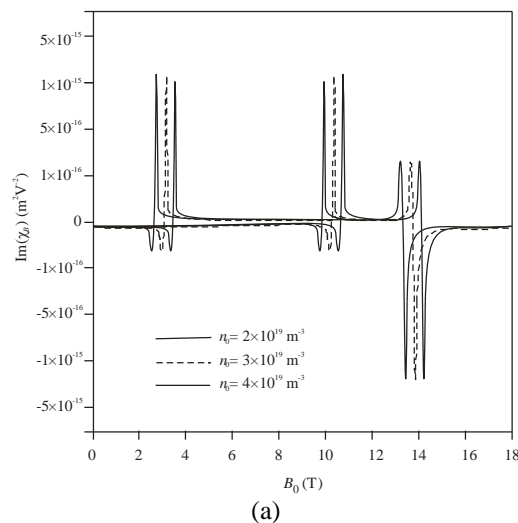


Figure 3(a) Variation of $\text{Im}(\chi_B)$ versus B_0 with excluding HCEs for the parameters given in **Figure (2a)**.

In **Figures (2a)** and **(2b)**, $\text{Re}(\chi_B)$ is plotted versus magnetic field B_0 with excluding and including HCEs, respectively for 3 different doping concentration ($n_0 = 2 \times 10^{19} \text{ m}^{-3}$, $3 \times 10^{19} \text{ m}^{-3}$ and $n_0 = 4 \times 10^{19} \text{ m}^{-3}$) at $E_0 = 7 \times 10^7 \text{ Vm}^{-1}$. These give a picture of the enhancement of $\text{Re}(\chi_B)$ as well as alter of its signs. For a fixed n_0 , the nature of curves is similar to as obtained in Figure 1a. An increase in n_0 does not alters the magnitude of peak positive and negative values of $\text{Re}(\chi_B)$, rather it shifts the value of B_0 at which change of sign of $\text{Re}(\chi_B)$ occurs towards lower values. A comparison between results of **Figures (2a)** and **(2b)** reveals that for a fixed n_0 , the HCEs induced by laser radiation widens the range of B_0 at which the change of sign of $\text{Re}(\chi_B)$ occurs; a result which supports the results of **Figure(1a)**.

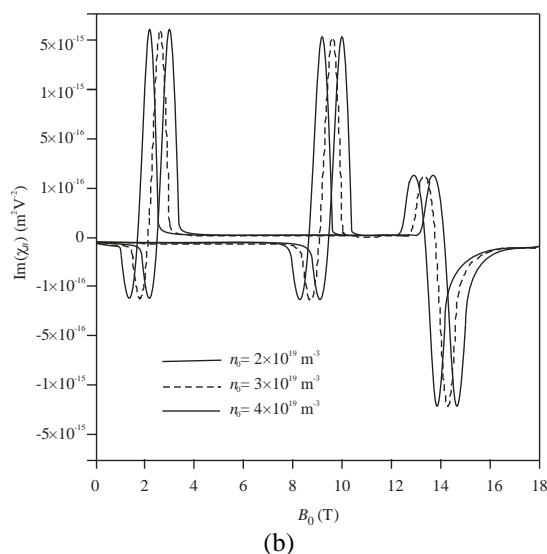


Figure 3(b) Variation of $\text{Im}(\chi_B)$ versus B_0 with including HCEs for the parameters given in **Figure (2a)**.

In **Figures (3a)** and **(3b)**, $\text{Im}(\chi_B)$ is plotted versus magnetic field B_0 with excluding and including HCEs, respectively for the parameters given in **Figures (2a)** and **(2b)**. These give a picture of the enhancement of $\text{Im}(\chi_B)$ as well as alter of its signs. For a fixed n_0 , the nature of curves is similar to as obtained in Figure 1b. An increase in n_0 does not alters the magnitude of peak positive and negative values of $\text{Im}(\chi_B)$, rather it shifts the value of B_0 at which change of sign of $\text{Im}(\chi_B)$ occurs towards lower values. A comparison between results of Figs. 3a and 3b reveals that for a fixed n_0 , the HCEs induced by intense laser radiation widens the range of B_0 at which the change of sign of $\text{Im}(\chi_B)$ occurs; a result which supports the results of **Figure(1b)**.

From Eqs. (22a) - (22b), it can be seen that apart from magnetic field dependence, laser radiation field strength can also be employed to enhance $\text{Re}, \text{Im}(\chi_B)$. In **Figure 4**, magnitudes of both $\text{Re}, \text{Im}(\chi_B)$ are plotted versus laser radiation field amplitude E_0 for the cases: (i) without HCEs, and (ii) with HCEs. It can be seen that both $\text{Re}, \text{Im}(\chi_B)$ exhibit the similar nature of curves throughout the plotted range of E_0 such that $\text{Re}(\chi_B) = 2.5 \text{Im}(\chi_B)$. When HCEs are included, the shape of the curve is a parabola. For smaller values of E_0 ($< 4 \times 10^7 \text{ Vm}^{-1}$) when HCEs insignificant, both $\text{Re}, \text{Im}(\chi_B)$ increases in a parabolic shape with increasing E_0 . However, they gradually start deviating from the parabolic shape as HCEs become significant, in the region $E_0 \geq 4 \times 10^7 \text{ Vm}^{-1}$. Both $\text{Re}, \text{Im}(\chi_B)$ become almost independent of E_0 beyond $E_0 \approx 10^8 \text{ Vm}^{-1}$ and as evident from this figure that both $\text{Re}, \text{Im}(\chi_B)$ become almost double when HCEs are included in comparison to when they are excluded. This behaviour can be easily understood in

terms of temperature dependence of $\text{Re}, \text{Im}(\chi_B)$ via MTCF of electrons in Eqs. (22a) - (22b). This deviation of Brillouin susceptibilities curves (from the parabolic shape) at high laser radiation field emphasis the necessity of inclusion of HCEs in SBS processes.

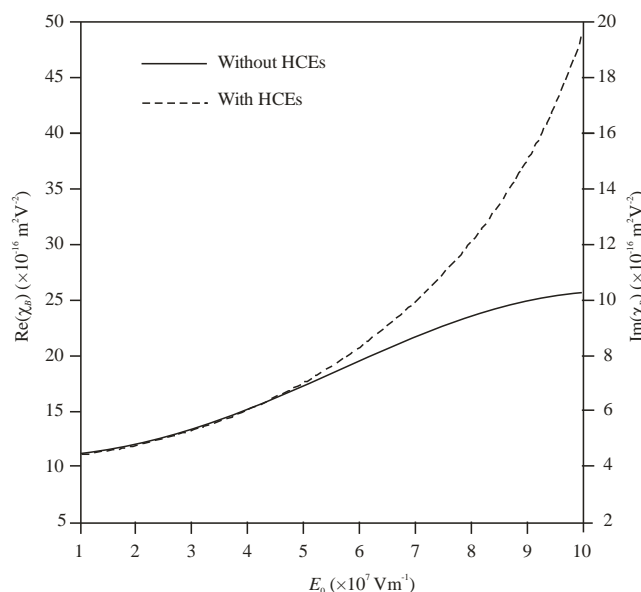


Figure 4 Variation of $\text{Re}, \text{Im}(\chi_B)$ versus E_0 at $B_0 \approx 14.2$ T for the cases (i) and (ii) given in **Figure(1a)**.

Conclusions

In the present paper, a theoretical formulation followed by numerical analysis is made to study HCEs on real and imaginary parts of Brillouin susceptibility of magnetoactive doped III-V semiconductors, applied to n-type doped InSb crystal. The analysis offer 3 achievable resonance conditions: (i) $(\omega_p^2 \omega_c^2) / v^2 \sim \omega_s^2$, (ii) $v^2 \omega_p^2 / (v^2 + \omega_c^2) \sim \omega_s^2$, and (iii) $\omega_c^2 \sim \omega_0^2$; at which significant enhancement as well as change of sign of $\text{Re}, \text{Im}(\chi_B)$ occur. Resonance conditions (i) and (ii) offer the tuning of scattered Stokes Brillouin mode over a wide range of frequencies by properly controlling the doping level and/or external magnetic field. The HCEs of intense laser radiation; (a) enhances the peak positive and negative values of $\text{Re}, \text{Im}(\chi_B)$ considerably, (b) shifts the enhanced peak positive and negative values of $\text{Re}, \text{Im}(\chi_B)$ towards lower values of magnetic field, and (c) widens the range of magnetic field at which the change of sign of $\text{Re}, \text{Im}(\chi_B)$ occur. For laser radiation field amplitude $E_0 < 4 \times 10^7 \text{ Vm}^{-1}$, HCEs on $\text{Re}, \text{Im}(\chi_B)$ are absent. However, for $E_0 \geq 4 \times 10^7 \text{ Vm}^{-1}$, HCEs become significant and more pronounced. The analysis establishes the technological potentiality of III-V semiconductors as the hosts for the fabrication of SBS dependent widely tunable and efficient optoelectronic devices such as optical switches and frequency converters.

Acknowledgements

Thankful to Professor S.K. Ghoshal, Department of Physics, Universiti Teknologi, Malaysia for many useful suggestions to carry out this work.

References

- [1] P Unsbo, F Saeidi and G Manneberg. Image formation in phase conjugation with large wavelength conversion. *J. Opt. Soc. Am.* 1993; **10**, 2532-8.
- [2] BI Stepanov, EV Ivakin and AG Rubanov. On recording flat and volume dynamical holograms. *Doklady Akademii Nauk SSSR* 1971; **196**, 567.
- [3] A Yariv and P Yeh. *Optical waves in crystals*. Propagation and Control of Laser Radiation. John Wiley & Sons, New York, 1984, p. 54-154.

- [4] G Banfi, V Degiorgio and D Ricard. Nonlinear optical properties of semiconductor nanocrystals. *Adv. Phys.* 1998; **47**, 447-510.
- [5] H Haug and SW Koch. *Quantum theory of the optical and electronic properties of semiconductors*. 5th ed. World Scientific, Singapore, 2004.
- [6] S Mokkalapati and C Jagadish. III-V compound SC for optoelectronic devices. *Mater. Today* 2009; **12**, 22-32.
- [7] E Garmire. Resonant optical nonlinearities in semiconductors. *IEEE J. Sel. Top. Quant. Electron.* 2000; **6**, 1094-110.
- [8] DAB. Miller. Dynamic nonlinear optics in semiconductors: Physics and applications. *Laser Focus World* 1983; **19**, 61-68.
- [9] S Sandeep, S Dahiya and N Singh. Parametric excitation of optical phonons in weakly polar narrow band gap magnetized semiconductor plasmas. *Mod. Phys. Lett. B* 2017; **31**, 1750294.
- [10] S Bhan, HP Singh, V Kumar and M Singh. Low threshold and high reflectivity of optical phase conjugate mode in transversely magnetized semiconductors. *Optik* 2019; **184**, 467-72.
- [11] E Garmire. Prospectives on stimulated Brillouin scattering. *New J. Phys.* 2017; **19**, 011003.
- [12] Z Bai, H Yuan, Z Liu, P Xu, Q Gao, RJ Williams, O Kitzler, RP Mildren, Y Wang and Z Lu. Stimulated Brillouin scattering materials, experimental design and applications. *Opt. Mater.* 2018; **75**, 626-45.
- [13] M Singh, P Aghamkar, N Kishore and PK Sen. Influence of piezoelectricity and magnetic field on stimulated Brillouin scattering in III-V semiconductors. *J. Nonlinear Opt. Phys. Mater.* 2006; **15**, 465-79.
- [14] P Aghamkar, M Singh, N Kishore, S Duhan and PK Sen. Steady-state and transient Brillouin gain in magnetoactive narrow band gap semiconductors. *Semicond. Sci. Tech.* 2007; **22**, 749-54.
- [15] M Singh and P Aghamkar. Mechanism of phase conjugation via stimulated Brillouin scattering in narrow bandgap semiconductors. *Optic. Comm.* 2008; **281**, 1251-5.
- [16] M Singh, P Aghamkar, N Kishore and PK Sen. Nonlinear absorption and refractive index of Brillouin scattered mode in semiconductor-plasmas by an applied magnetic field. *Optic. Laser Tech.* 2008; **40**, 215-22.
- [17] C Uzma, I Zeba, HA Shah and M Salimullah. Stimulated Brillouin scattering of laser radiation in a piezoelectric semiconductor: Quantum effect. *J. Appl. Phys.* 2009; **105**, 013307.
- [18] E Garmire. Stimulated Brillouin review: Invented 50 years ago and applied today. *Int. J. Optic.* 2018; **2018**, 2459501.
- [19] SG Chefranov and AS Chefranov. *Hydrodynamic methods and exact solutions in applications to the electromagnetic field theory in medium*. In: BI Lembrikov (Ed.). *Nonlinear Optics - Novel Results in Theory and Applications*. Intech Open, London, 2018.
- [20] GC Aers and AD Boardman. The theory of semiconductor magnetoplasmon-polariton surface modes: Voigt geometry. *J. Phys. C Solid State Phys.* 1978; **11**, 945-59.
- [21] G Sharma and S Ghosh. Parametric excitation and amplification of an acoustic wave in a magnetized piezoelectric semiconductor. *Phys. Status Solidi* 2001; **184**, 443-52.
- [22] AC Beer. *Galvanometric effects in semiconductors: Solid state physics*. Academic Press, New York, 1963.
- [23] GJ Pert. *Self focusing of laser beams in dielectrics, plasmas and semiconductors*. *Phys. Bull.* 1975; **26**; 225.
- [24] EM Conwell. *High field transport in semiconductors*. Academic Press, New York, 1967.
- [25] N Nimje, S Dubey and S Ghosh. Parametric interaction in acousto-optical semiconductor plasmas in the presence of hot carriers. *Chin. J. Phys.* 2011; **49**, 901-16.
- [26] VE Gusev and AA Karabutov. *Laser optoacoustics*. American Institute of Physics, New York, 1993.
- [27] PY Yu and M Cardona. *Vibrational properties of semiconductors, and electron-phonon interactions*. Fundamentals of Semiconductors. Springer, Germany, 2010.
- [28] ED Palik and JK Furdyna. Infrared and microwave magnetoplasma effects in semiconductors. *Rep. Progr. Phys.* 1970; **33**, 1193-322.
- [29] ER Generazio and HN Spector. Free-carrier absorption in quantizing magnetic fields. *Phys. Rev. B.* 1979; **20**, 5162-7.